# Wave functions and edge states in rectangular honeycomb lattices revisited: Nanoflakes, armchair and zigzag nanoribbons, and nanotubes

Anton Talkachov [*] and Egor Babaev
*Department of Physics, KTH-Royal Institute of Technology, SE-10691 Stockholm, Sweden*

Properties of bulk and boundaries of materials can, in general, be quite different, both for topological and nontopological reasons. One of the simplest boundary problems to pose is the tight-binding problem of noninteracting electrons on a finite honeycomb lattice. Despite its simplicity, the problem is quite rich and directly related to the physics of graphene. We revisit this long-studied problem and present an analytical derivation of the electron spectrum and wave functions for graphene rectangular derivatives. We provide an exact analytical description of extended and localized states, the transition between them, and a special case of a localized state when the wave function is nonzero only at the edge sites. The latter state has zero energy, and we discuss its existence in zigzag nanoribbons, zigzag nanotubes with a number of sites along a zigzag edge divisible by 4, and rectangular graphene nanoflakes with an odd number of sites along both zigzag and armchair edges.

## I. INTRODUCTION

The successive downscaling of graphene-based devices with atomic level precision [1] shows the significant effect of edges on the electronic structure of graphene [2], which has experimental evidence [3–5]. Insights into the electronic properties of graphene and its derivatives can be obtained from exact analytical approaches. There are two basic approaches for describing rectangular structures: based on the division of graphene into two sublattices [6–12] (equivalently, choosing two atom unit cells), or choosing a unit cell consisting of four atoms [13–17]. The first one is usually applied when describing infinite systems and nanoribbons, while the second one is used mostly for finite systems. There are also two basic edge shapes for nanoribbons: armchair and zigzag. It has been shown that zigzag nanoribbons possess localized edge states with energies close to the Fermi level [7–9,11,18,19]. The edge states have been predicted to be important in transport [20], electromagnetic [21], and optical properties [11,22]. In contrast, edge states are absent for armchair nanoribbons [2,7,8]. The same results have been shown from the topological point of view [23]. Besides graphene, the problem is also relevant for artificial honeycomb structures and ultracold atoms on honeycomb optical lattices.

We revisit the basic problem of $\pi$ electrons in rectangular graphene geometries (armchair and zigzag nanoribbons, nanotubes, finite samples). We establish the transition points between extended and localized states. It is often assumed that these points can be treated with wave functions for extended waves [7,8,12–14,17]. However, we show that the direct approach leads to a trivial (zero) wave function everywhere and we need to take the limit to these points from the left and the right. We discuss that at these transitions, wave functions have a linear dependence on the site index. We also describe the two entirely localized zero energy states with nonzero wave functions only at the edge sites for zigzag nanoribbons, zigzag nanotubes, and one geometry of rectangular graphene nanoflake, that to the best of our knowledge were not reported before. We discuss wave functions in a rectangular graphene system, including expressions for localized states.

This paper is organized as follows. In Sec. II, we recap the eigenvalue problem for the infinite honeycomb lattice, where wave functions are running waves in both $x$ and $y$ directions. In Sec. III, we switch to problems for finite system size in one direction: armchair and zigzag nanoribbons and nanotubes. Here we show that edge states are realizable only for nanoribbons and nanotubes with zigzag open edges. Importantly, there is an entirely localized edge state with zero energy, where wave functions are nonzero only at the edge sites. In Sec. IV, we find wave functions for extended and localized states in a finite sample with rectangular geometry. We show analytically that there is only one possible geometry which allows for an entirely localized edge state.

## II. THE INFINITE SYSTEM

Let us first look at the infinite honeycomb structure made from identical atoms. We divide these atoms into two groups $(A, B)$ which form triangular lattices (Fig. 1). The effective
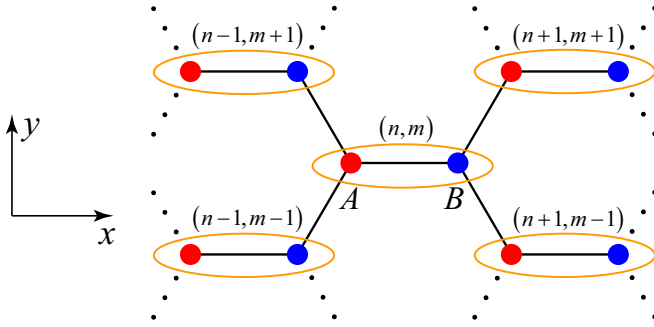
---

*anttal@kth.se

FIG. 1. The honeycomb lattice in real space, where the red (blue) circles mean an $A$ ($B$) sublattice site.

Hamiltonian for the system reads

$$H_{\text{eff}} = -t \sum_{\langle \mathbf{i,j} \rangle} (a_{\mathbf{i}}^{\dagger} b_{\mathbf{j}} + b_{\mathbf{j}}^{\dagger} a_{\mathbf{i}}). \quad (1)$$

Here, $a_{\mathbf{i}}^{\dagger}(a_{\mathbf{i}})$ is the creation (annihilation) operator for an electron on site $A$ in the cell whose position is described by the vector $\mathbf{i} = (n, m)$, where $n$ ($m$) specifies the horizontal (vertical) position with indexation illustrated in Fig. 1. The same applies to operators $b_{\mathbf{i}}^{\dagger}$ and $b_{\mathbf{i}}$, which correspond to sites $B$. This Hamiltonian describes kinetic energy (hopping between nearest-neighbor sites $\langle \mathbf{i, j} \rangle$ without spin flip), parameterized by the hopping integral $t$ ($t > 0$ and assumed to be constant in space). A general state can be written as

$$|\Psi\rangle = \sum_{\mathbf{i}} (\psi_{A,\mathbf{i}} a_{\mathbf{i}}^{\dagger} + \psi_{B,\mathbf{i}} b_{\mathbf{i}}^{\dagger}) |0\rangle, \quad (2)$$

where $\psi_{A,\mathbf{i}}$ ($\psi_{B,\mathbf{i}}$) is the real space wave function describing an electron on the $A$ ($B$) sublattice, and $|0\rangle$ denotes the vacuum state with no particle present. We will assume the plane wave form of the wave functions,

$$\begin{pmatrix} \psi_{A,\mathbf{i}} \\ \psi_{B,\mathbf{i}} \end{pmatrix} = e^{i(k_x n + k_y m)} \begin{pmatrix} f_A(\mathbf{k}) \\ f_B(\mathbf{k}) \end{pmatrix}, \quad (3)$$

and we come to the Schrödinger equation,

$$H_{\text{eff}} |\Psi\rangle = E |\Psi\rangle, \quad (4)$$

which takes the form

$$\begin{pmatrix} 0 & -t(1 + 2e^{-ik_x} \cos k_y) \\ -t(1 + 2e^{ik_x} \cos k_y) & 0 \end{pmatrix} \begin{pmatrix} f_A(\mathbf{k}) \\ f_B(\mathbf{k}) \end{pmatrix}$$
$$= E \begin{pmatrix} f_A(\mathbf{k}) \\ f_B(\mathbf{k}) \end{pmatrix}. \quad (5)$$

Eigenvalues of the matrix in this equation give possible energies:

$$E_s = s \cdot t \cdot \epsilon(k_x, k_y),$$
$$\epsilon(k_x, k_y) = \sqrt{3 + 4 \cos k_x \cos k_y + 2 \cos 2k_y}, \quad (6)$$

where we have introduced the parameter $s = \pm 1$ to distinguish between valence ($-1$) and conduction ($+1$) bands. The corresponding eigenvectors $(f_A(\mathbf{k}), f_B(\mathbf{k}))^T$ allow us to calculate normalized wave functions (3) for the infinite honeycomb

lattice:

$$\begin{pmatrix} \psi_{A,\mathbf{i}} \\ \psi_{B,\mathbf{i}} \end{pmatrix} = \frac{1}{\sqrt{2}} e^{i(k_x n + k_y m)} \begin{pmatrix} -\frac{s(1 + 2e^{-ik_x} \cos k_y)}{\epsilon(k_x, k_y)} \\ 1 \end{pmatrix}. \quad (7)$$

Note that $\psi_{A,\mathbf{i}}$ and $\psi_{B,\mathbf{i}}$ is only a basis. General wave functions that describe the system are superpositions of all these possible states.

## III. SYSTEMS FINITE IN ONE DIRECTION

### A. Wave functions for armchair nanoribbons and nanotubes

An armchair nanoribbon is a sample of the honeycomb lattice arranged as in Fig. 2, which is finite in $y$. Wave functions, in this case, can be obtained as a superposition of traveling waves in $+y$ and $-y$ directions:

$$\begin{pmatrix} \psi_{A,\mathbf{i}} \\ \psi_{B,\mathbf{i}} \end{pmatrix} = \left[ c_1 \frac{1}{\sqrt{2}} \begin{pmatrix} -\frac{s(1 + 2e^{-ik_x} \cos k_y)}{\epsilon(k_x, k_y)} \\ 1 \end{pmatrix} e^{ik_y m} \right.$$
$$\left. + c_2 \frac{1}{\sqrt{2}} \begin{pmatrix} -\frac{s(1 + 2e^{-ik_x} \cos(-k_y))}{\epsilon(k_x, -k_y)} \\ 1 \end{pmatrix} e^{i(-k_y)m} \right] e^{ik_x n}$$
$$= \frac{1}{\sqrt{2}} \begin{pmatrix} -\frac{s(1 + 2e^{-ik_x} \cos k_y)}{\epsilon(k_x, k_y)} \\ 1 \end{pmatrix} [c_1 e^{ik_y m} + c_2 e^{-ik_y m}] e^{ik_x n}, \quad (8)$$

where $c_1$ and $c_2$ are normalization constants. These wave functions should satisfy open boundary conditions (some authors [19] say that the dangling bonds at the edge are terminated by hydrogen atoms so they do not contribute to the electronic states):

$$\begin{pmatrix} \psi_{A,\mathbf{i}=(n,0)} \\ \psi_{B,\mathbf{i}=(n,0)} \end{pmatrix} = \begin{pmatrix} 0 \\ 0 \end{pmatrix}, \quad \begin{pmatrix} \psi_{A,\mathbf{i}=(n,N_y+1)} \\ \psi_{B,\mathbf{i}=(n,N_y+1)} \end{pmatrix} = \begin{pmatrix} 0 \\ 0 \end{pmatrix}. \quad (9)$$

Physically, this means that electrons are absent outside the considered system (their wave function equals zero). This leads to the following relation between $c_1$ and $c_2$, and to the possible values of wave number $k_y$:

$$c_2 = -c_1, \quad k_y = \frac{\pi j_y}{N_y + 1}, \quad j_y = 1, 2, 3, \ldots, N_y. \quad (10)$$

Wave number $k_x$ should be treated as a continuous variable in the case of an infinite honeycomb sheet in the $x$ direction. We consider a case of a honeycomb nanotube with open armchair boundaries ($N_x$ has to be even). For this case we use periodic boundary conditions along the $x$ axis: $\psi_{A,\mathbf{i}=(n,m)} = \psi_{A,\mathbf{i}'=(n+N_x,m)}$, $\psi_{B,\mathbf{i}=(n,m)} = \psi_{B,\mathbf{i}'=(n+N_x,m)}$. This leads to a discrete set of $k_x$ values:

$$k_x = \frac{2\pi}{N_x} v_x, \quad v_x = 0, 1, 2, \ldots, \frac{N_x}{2} - 1. \quad (11)$$

A system consists of $N_x N_y$ sites, so the eigenvalue problem [Eq. (4)] should have $N_x N_y$ different eigenvalues and eigenvectors. We have $N_y$ values of $k_y$ [Eq. (10)], $N_x/2$ values of $k_x$ [Eq. (11)], and two different values of the parameter $s = \pm 1$. The coefficient $c_1$ can be found from the following
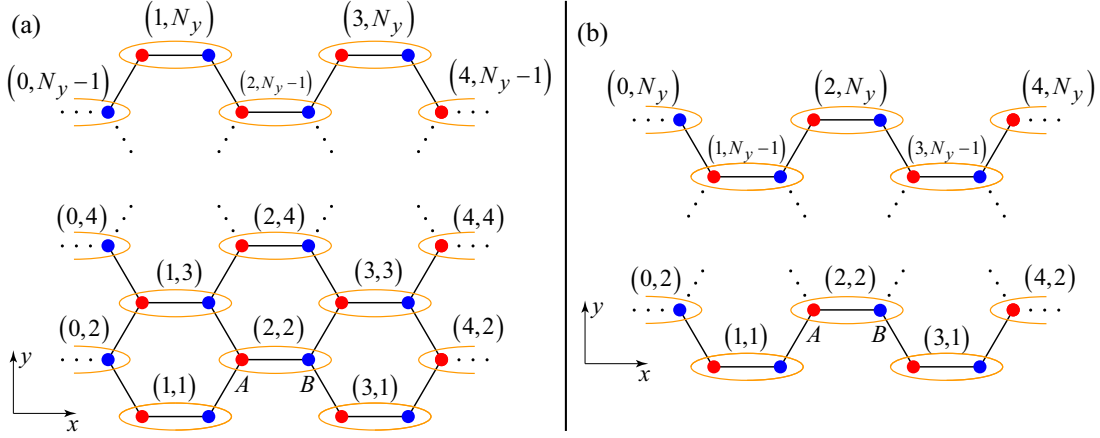
FIG. 2. Honeycomb lattice with armchair edges (armchair nanoribbon) in two different cases: (a) $N_y$ is odd, (b) $N_y$ is even.

normalization conditions:

$$\sum_{\mathbf{i}} (\psi_{A,\mathbf{i}}, \psi_{B,\mathbf{i}})(\psi_{A,\mathbf{i}}, \psi_{B,\mathbf{i}})^{\dagger} = 1,$$

$$\sum_{s,k_x,k_y} (\psi_{A,\mathbf{i}}, \psi_{B,\mathbf{i}})(\psi_{A,\mathbf{i}}, \psi_{B,\mathbf{i}})^{\dagger} = 1. \tag{12}$$

In the article, we always use the first of the rules to find the normalization coefficients, but the second one is also satisfied in all considered cases. The constant $c_1$ has the form

$$c_1 = -i[2N_x \cdot S(k_y, N_y)]^{-1/2}, \tag{13}$$

$$S(k, N) = \sum_{m=1}^{N} \sin^2 km = \frac{1}{2}\left[N - \frac{\sin kN}{\sin k}\cos k(N+1)\right], \tag{14}$$

where we have introduced auxiliary function $S(k, N)$. Note that this normalization coefficient is defined up to an arbitrary factor $e^{i\phi}$, which is why wave functions from Refs. [7,8,15,24] may look different from our final result:

$$\begin{pmatrix} \psi_{A,\mathbf{i}} \\ \psi_{B,\mathbf{i}} \end{pmatrix} = \frac{e^{ik_x n}\sin k_y m}{\sqrt{N_x \cdot S(k_y, N_y)}}\begin{pmatrix} -\frac{s(1+2e^{-ik_x}\cos k_y)}{\epsilon(k_x,k_y)} \\ 1 \end{pmatrix}. \tag{15}$$

After renormalization, the results become identical. These states are called extended because they describe waves which extend over the whole ribbon width. Our way of presenting results is better for computer-based calculations, in comparison with using square roots from complex numbers [7,8] which are multivalued functions.

There is a zero energy state for armchair nanoribbons of width $N_y = 3r - 1$ (where $r = 1, 2, 3, \ldots$) at $k_x = 0$, $k_y = 2\pi/3$ (see band structure for infinite ribbon in Fig. 3). The system with such a width in the $y$ direction is called metallic [18,19]. The wave function for $A$ sites is ill-defined at the point, because there exists the following $\frac{0}{0}$ uncertainty:

$$\lim_{k_x \to 0, k_y \to 2\pi/3} \frac{1 + 2e^{-ik_x}\cos k_y}{\epsilon(k_x, k_y)}$$

$$= \lim_{k_x \to 0, k_y \to 2\pi/3} \frac{ik_x - \sqrt{3}(k_y - 2\pi/3)}{\sqrt{k_x^2 + 3(k_y - 2\pi/3)^2}} = e^{i\varphi}, \tag{16}$$

where we have introduced the parameter $\varphi \in [0; 2\pi)$ which depends on the ratio $k_x/(k_y - 2\pi/3)$. The possible values of wave number $k_y$ [Eq. (10)] are obtained from the boundary conditions. The wave number $k_x$ is either a continuous variable for an infinite nanoribbon or is quantized [Eq. (11)] due to periodic boundary conditions for armchair nanotubes. One can see that $k_x$ and $k_y$ are independent, and consequently, $\varphi$ is arbitrary and can be chosen artificially. It is convenient to choose $\varphi = \pi$, then wave functions at the point $k_x = 0$, $k_y = 2\pi/3$ have the form

$$\begin{pmatrix} \psi_{A,\mathbf{i}} \\ \psi_{B,\mathbf{i}} \end{pmatrix} = \frac{\sin(2\pi m/3)}{\sqrt{N_x \cdot S(2\pi/3, N_y)}}\begin{pmatrix} s \\ 1 \end{pmatrix}. \tag{17}$$

The zero energy state should be referred to as a bulk state, in contrast to localized states near zero energy for zigzag nanoribbons, which will be discussed in the next subsection.

### B. Wave functions for zigzag nanoribbons and nanotubes

Zigzag nanoribbons are systems that are finite in the $x$ direction but can be infinite in the $y$ direction (Fig. 4).

Let us apply an approach similar to the previous subsection: obtain wave functions as a superposition of waves
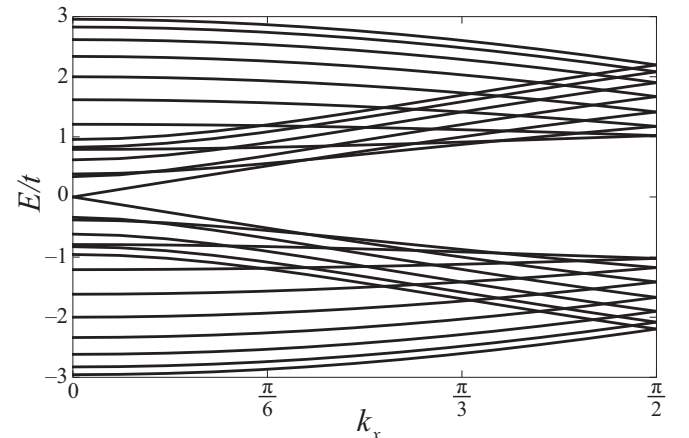


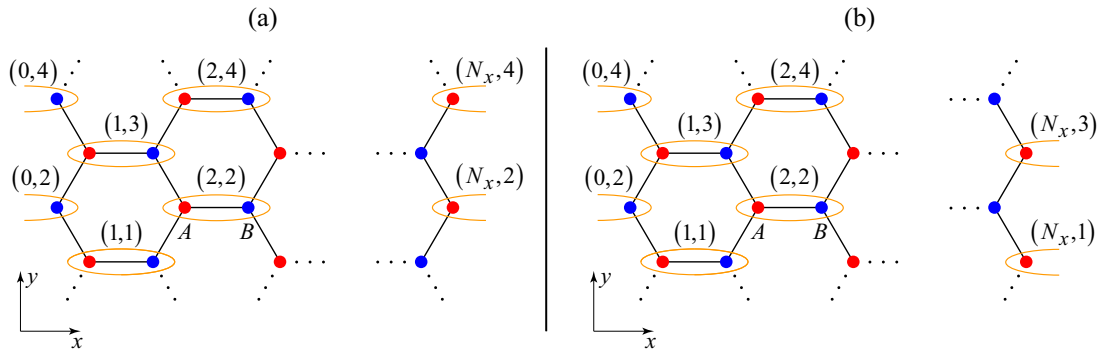FIG. 3. Band structure of the infinite armchair ribbon for $N_y = 14$.

FIG. 4. Honeycomb lattice with zigzag edges (zigzag nanoribbon) in two different cases: (a) $N_x$ is even, (b) $N_x$ is odd.

traveling in $\pm x$ directions:

$$
\begin{pmatrix} \psi_{A,\mathbf{i}} \\ \psi_{B,\mathbf{i}} \end{pmatrix} = \left[ c_3 \frac{1}{\sqrt{2}} \begin{pmatrix} -\frac{s(1+2e^{-ik_x}\cos k_y)}{\epsilon(k_x,k_y)} \\ 1 \end{pmatrix} e^{ik_x n} + c_4 \frac{1}{\sqrt{2}} \begin{pmatrix} -\frac{s(1+2e^{-i(-k_x)}\cos k_y)}{\epsilon(-k_x,k_y)} \\ 1 \end{pmatrix} e^{i(-k_x)n} \right] e^{ik_y m}
$$

$$
= \frac{1}{\sqrt{2}} \left[ c_3 \begin{pmatrix} -\frac{s(1+2e^{-ik_x}\cos k_y)}{\epsilon(k_x,k_y)} \\ 1 \end{pmatrix} e^{ik_x n} + c_4 \begin{pmatrix} -\frac{s(1+2e^{ik_x}\cos k_y)}{\epsilon(k_x,k_y)} \\ 1 \end{pmatrix} e^{-ik_x n} \right] e^{ik_y m}, \tag{18}
$$

where $c_3$ and $c_4$ are coefficients that can be found from normalization conditions (12). Wave functions (18) satisfy the following boundary conditions:

$$
\psi_{A,\mathbf{i}=(0,m)} = 0, \quad \psi_{B,\mathbf{i}=(N_x,m)} = 0. \tag{19}
$$

These constraints lead to

$$
\sin k_x N_x + 2 \cos k_y \sin [k_x(N_x + 1)] = 0, \tag{20}
$$

$$
c_2 = -c_1 e^{2ik_x N_x}. \tag{21}
$$

Possible values for wave number $k_y$ are obtained using the assumption of periodic boundary conditions in the $y$ direction (honeycomb nanotube with open zigzag edges): $\psi_{A,\mathbf{i}=(n,m)} = \psi_{A,\mathbf{i}'=(n,m+N_y)}$, $\psi_{B,\mathbf{i}=(n,m)} = \psi_{B,\mathbf{i}'=(n,m+N_y)}$. In this case, the number of sites in the $y$ direction ($N_y$) has to be even. The wave number satisfies

$$
k_y = \frac{2\pi}{N_y} \nu_y, \quad \nu_y = 0, 1, 2, \ldots, \frac{N_y}{2} - 1. \tag{22}
$$

The transcendental Eq. (20) contains $N_x$ different roots for the wave number $k_x$. This equation has $N_x$ real nontrivial roots in the region $k_x \in (0; \pi)$ for $k_y \in [0; k_y^c] \cup (\pi - k_y^c; \pi]$ and $N_x - 1$ real roots otherwise, where

$$
k_y^c = \arccos \frac{N_x}{2(N_x + 1)}. \tag{23}
$$

The other one in the latter case is a complex solution. It can be obtained numerically, analytically using approximate formulas [14], or using fitting formulas for roots [10] that are obtained from numerical results. Values of the wave number $k_x = 0$ and $\pm\pi$ are called unphysical [8], because they lead to a trivial wave function which equals zero at all sites. The equation is similar to one that was applied to graphene nanoribbons with an additional methylene group at every edge site [25], so this problem has been known for a long time.

The band structure of an infinite zigzag ribbon is presented in Fig. 5 to help the reader visualize regions and points of

the next subsections. Region $k_y \in (\frac{\pi}{2}; \pi)$ is omitted due to the symmetry of the energy band $[E(\tilde{k}_x, \pi - k_y) = E(k_x, k_y)]$. Lines transform to a set of points for nanotubes on the band structure.

### 1. Case $k_y \in [0; k_y^c] \cup (\pi - k_y^c; \pi]$

In this case, all roots are real and can be found numerically from Eq. (20). Corresponding wave functions describe extended states:

$$
\begin{pmatrix} \psi_{A,\mathbf{i}} \\ \psi_{B,\mathbf{i}} \end{pmatrix} = -\sqrt{2} i c_3 e^{i(k_x N_x + k_y m)} \begin{pmatrix} s_1 s \sin(k_x n) \\ \sin[k_x(N_x - n)] \end{pmatrix}, \tag{24}
$$

$$
s_1 = \frac{\sqrt{\sin^2 k_x}}{\sin k_x} \cdot \frac{\sin[k_x(N_x + 1)]}{\sqrt{\sin^2[k_x(N_x + 1)]}} = \text{sign}\{\sin[k_x(N_x + 1)]\}. \tag{25}
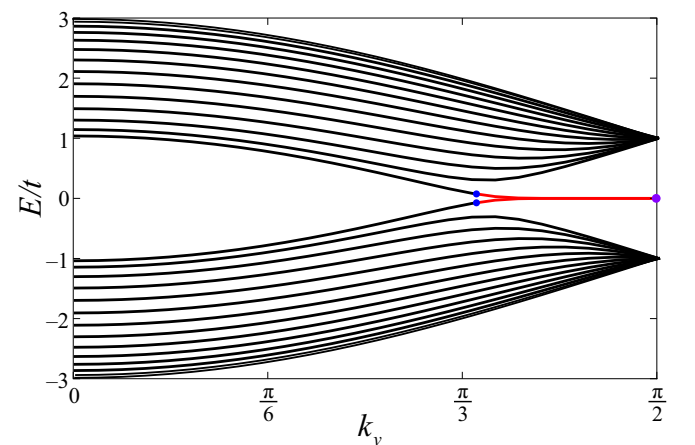$$



FIG. 5. Band structure of the infinite zigzag ribbon for $N_x = 14$. Black and red lines correspond to bulk and edge states, respectively. Blue and purple points indicate transition points and the entirely localized state, respectively.

The sign function $s_1$ can be simplified if one introduces special indexation for $k_x$ roots to distinguish different subbands [7,11]. The normalization constant $c_3$ can be written in the following way:

$$c_3 = ie^{-ik_x N_x}[2N_y \cdot S(k_x, N_x)]^{-1/2}, \qquad (26)$$

where the complex factor is chosen in this form to have a compact presentation for the wave functions:

$$\begin{pmatrix} \psi_{A,\mathbf{i}} \\ \psi_{B,\mathbf{i}} \end{pmatrix} = \frac{e^{ik_y m}}{\sqrt{N_y \cdot S(k_x, N_x)}} \begin{pmatrix} s_1 s \sin(k_x n) \\ \sin[k_x(N_x - n)] \end{pmatrix}. \qquad (27)$$

Similar results were obtained in Refs. [7,8,10,11]. However, there is no sign function depending on $k_x$ in Refs. [8,10]. The authors of Ref. [8] corrected the mistake in a later article [7] where, due to special numeration of roots of Eq. (20) $k_x^r$, a factor of $(-1)^r$ appears in wave functions which play the same role as the function $s_1$ [Eq. (25)] in our representation. Their index $r$ is related to the band number in Ref. [7]. In Ref. [11], wave functions were derived in the limit $k_y \to 0$. They coincide with our wave functions (27) for $k_y = 0$.

Existence of the sign function $s_1$ [or similar factor $(-1)^r$ to divide subbands] reflects inversion symmetry of the electron wave function and plays an important role for the optical selection rules [11,26].

### 2. Case $k_y \in (k_y^c; \frac{\pi}{2}) \cup (\frac{\pi}{2}; \pi - k_y^c)$

In this case $N_x - 1$ real roots for $k_x$ can be found from Eq. (20), and the corresponding wave functions have the form of Eq. (27). One more root can be obtained by analytical continuation to the complex plane [8],

$$k_x \to \begin{cases} \pi \pm ik_x', & k_y \in \left(k_y^c; \frac{\pi}{2}\right), \\ 0 \pm ik_x', & k_y \in \left(\frac{\pi}{2}; \pi - k_y^c\right), \end{cases} \qquad (28)$$

and describes the edge state which corresponds to wave functions localized in space. For $k_y = \frac{\pi}{2}$ we need to obtain solutions separately, and we will do this later. With the ansatz Eq. (28), the function $\epsilon(k_x, k_y)$ inside eigenenergies $E_s$ (6) and transcendental Eq. (20) transform to

$$\epsilon(k_x', k_y) = \begin{cases} \sqrt{3 - 4\cosh k_x' \cos k_y + 2\cos 2k_y}, & k_y \in \left(k_y^c; \frac{\pi}{2}\right), \\ \sqrt{3 + 4\cosh k_x' \cos k_y + 2\cos 2k_y}, & k_y \in \left(\frac{\pi}{2}; \pi - k_y^c\right), \end{cases} \qquad (29)$$

$$\begin{cases} \sinh k_x' N_x - 2\cos k_y \sinh[k_x'(N_x + 1)] = 0, & k_y \in \left(k_y^c; \frac{\pi}{2}\right), \\ \sinh k_x' N_x + 2\cos k_y \sinh[k_x'(N_x + 1)] = 0, & k_y \in \left(\frac{\pi}{2}; \pi - k_y^c\right). \end{cases} \qquad (30)$$

Equation (30) contains two opposite roots. But after substituting them to find wave functions and normalizing, one can see that these roots describe identical wave functions with coinciding energies. Therefore, we are looking for only one (positive) root, which is to be found numerically. Both parts of Eq. (30) can be joined to one [8], which has the form

$$\sinh k_x' N_x - 2|\cos k_y| \sinh[k_x'(N_x + 1)] = 0. \qquad (31)$$

We need to obtain wave functions after finding all values of $k_y$ from Eq. (22), and the corresponding $k_x$ and energies. Related wave functions that describe complex solutions for $k_y \in (\frac{\pi}{2}; \pi - k_y^c)$ do not contain a sign function, but there is a sign function $(-1)^n$ depending on horizontal position for $k_y \in (k_y^c; \frac{\pi}{2})$:

$$\begin{pmatrix} \psi_{A,\mathbf{i}} \\ \psi_{B,\mathbf{i}} \end{pmatrix} = \sqrt{2}c_3' e^{-k_x' N_x + ik_y m} \begin{pmatrix} s \sinh(k_x' n) \\ \sinh[k_x'(N_x - n)] \end{pmatrix}$$
$$\cdot \begin{cases} (-1)^n, & k_y \in \left(k_y^c; \frac{\pi}{2}\right), \\ 1, & k_y \in \left(\frac{\pi}{2}; \pi - k_y^c\right). \end{cases} \qquad (32)$$

Their derivation is located in Appendix A. It is convenient to present the normalization constant $c_3'$ in the following way:

$$c_3' = e^{k_x' N_x}[2N_y \cdot S_{\mathrm{hyp}}(k_x', N_x)]^{-1/2}, \qquad (33)$$

where

$$S_{\mathrm{hyp}}(k, N) = \sum_{m=1}^{N} \sinh^2 km$$
$$= \frac{1}{4}\left[\frac{\sinh k(2N + 1)}{\sinh k} - (2N + 1)\right]. \qquad (34)$$

Wave functions (32) can be finally written as

$$\begin{pmatrix} \psi_{A,\mathbf{i}} \\ \psi_{B,\mathbf{i}} \end{pmatrix} = \frac{e^{ik_y m}}{\sqrt{N_y \cdot S_{\mathrm{hyp}}(k_x', N_x)}} \begin{pmatrix} s \sinh(k_x' n) \\ \sinh[k_x'(N_x - n)] \end{pmatrix}$$
$$\cdot \begin{cases} (-1)^n, & k_y \in \left(k_y^c; \frac{\pi}{2}\right), \\ 1, & k_y \in \left(\frac{\pi}{2}; \pi - k_y^c\right). \end{cases} \qquad (35)$$

Comparing the result to others, one can see that in Ref. [8] for the case $k_y \in (k_y^c; \frac{\pi}{2})$ in some formulas [Eqs. (B.40) and (23) in referenced article] the sign function exists in the form $e^{i\pi n}$ (converting to our type of numeration), but in some formulas [Eq. (B.44)] it is absent. Factor $e^{i\pi n}$ in Ref. [8] plays the same role as factor $(-1)^n$ in our Eq. (35). For the case $k_y \in (\frac{\pi}{2}; \pi - k_y^c)$, they also obtained results without the sign function.

In Ref. [7], authors work with $k_y$ in the range $(-\pi/2; \pi/2)$. They have continuation to the complex plane of one type $(k_x = \pi \pm ik_x')$, and it is right for their choice of $k_y$. However, they obtained localized wave functions with an extra sign function which depend on indexation of $k_x$ roots (as was explained in the previous subsection), which is incorrect (the vanishing procedure is described in Appendix A).

In Ref. [11] the range and possible values of $k_y$ are not specified, but from figures one can see that they used $k_y \in (-\pi/2; \pi/2)$ (in our notation). They used the transfer matrix method, and in the step when introducing a new variable in Eq. (11), they chose a sign that led to a changing sign of one term in the energy Eq. (14) and transcendental Eq. (19). Further, they chose the continuation of $k_x = 0 \pm i k_x'$, which is correct for their equation type. They obtained a result identical to our Eq. (35) for $k_y \in (\frac{\pi}{2}; \pi - k_y^c)$ with the same type of continuation.

### 3. Case $k_y = \pi/2$

To the best of our knowledge, previous papers dedicated to analytical calculations of localized wave functions in the honeycomb lattice, e.g., Refs. [8,11], do not discuss this special value of $k_y$ (or write that this value is included in the range of the previous subsection and wave functions should be treated with formulas (35) [7]). There are two papers [20,27] which discuss wave functions, but only for the zero energy modes described in the subsection. Below we will show that at this point wave functions should be derived more carefully.

For this value of wave number $k_y$, Eq. (20) simplifies to

$$\sin k_x N_x = 0, \tag{36}$$

leading to $N_x - 1$ real roots, which can be found analytically:

$$k_x = \frac{\pi}{N_x} j_x, \quad j_x = 1, 2, 3, \ldots, N_x - 1. \tag{37}$$

As in previous cases, we expect to have one eigenvalue that describes a localized state because on the $k_y$ axis this case is bounded from the left and the right by localized types of solutions for the eigenvalue problem. A straightforward method for finding solution $k_x$ in the complex plane leads to trivial nonphysical results $k_x = 0, \pi$. We find the solution for this case as a limit for the previous subsection's results.

First, we consider the left-hand limit, $k_y = \frac{\pi}{2} - \eta$, where $\eta \to 0^+$. In this case the complex plane continuation has the form $k_x = \pi \pm i k_x'$. There is a numerically obtained tendency: decreasing $\eta$ leads to increasing the imaginary part of $k_x$. The eigenvalue equation [first part of Eq. (30)] transforms to

$$\frac{1}{2} e^{k_x' N_x} - 2 \cos\left(\frac{\pi}{2} - \eta\right) \cdot \frac{1}{2} e^{k_x'(N_x+1)} = 0, \tag{38}$$

which is obtained in the limit $\eta \to 0$ ($k_x' \to \infty$). This has one solution,

$$k_x' = -\ln 2\eta, \tag{39}$$

which tends to infinity when $\eta \to 0$, confirming our numerical results.

The function $\epsilon(k_x', \frac{\pi}{2})$ [Eq. (29)] inside eigenenergies $E_s$ now can be written as

$$\epsilon\left(k_x', \frac{\pi}{2}\right) = \sqrt{3 - 4 \cdot \frac{1}{2} e^{k_x'} \cos k_y + 2\cos 2k_y}$$

$$= \lim_{\eta \to 0} \sqrt{3 - 2e^{-\ln 2\eta} \cos\left(\frac{\pi}{2} - \eta\right) + 2\cos 2\left(\frac{\pi}{2} - \eta\right)}$$

$$= \lim_{\eta \to 0} \sqrt{3 - 2 \cdot (2\eta)^{-1}\eta + 2 \cdot (-1)} = 0. \tag{40}$$
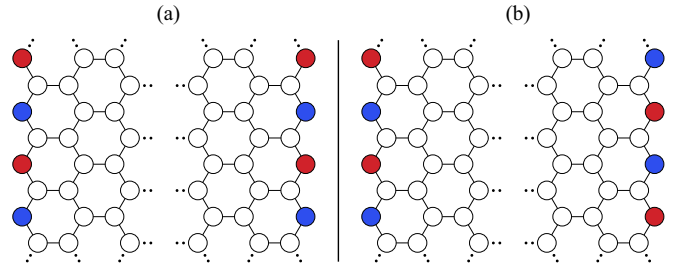


FIG. 6. Wave function of zigzag nanoribbon in entirely localized state [Eq. (43)] for even $N_x$: (a) conduction band and (b) valence band. The amplitudes are normalized by the maximum value of the respective wave functions. Here blue, white, and red correspond to amplitudes $-1$, $0$, and $1$, respectively.

Therefore, one of the wave numbers $k_x$ at this special point $k_y = \pi/2$ describes a zero energy state. This state has double degeneracy, because there are two different wave functions previously related to valence and conduction bands describing the one energy state. Before finding the explicit form of the wave functions in this case, let us first simplify the summation function (34) in our limit:

$$S_{\text{hyp}}(k_x', N_x) = \frac{1}{4}\left(\frac{\exp k_x'(2N_x + 1)}{\exp k_x'} - (2N_x + 1)\right)$$

$$= \lim_{\eta \to 0} \frac{1}{4}\left(\frac{(2\eta)^{-(2N_x+1)}}{(2\eta)^{-1}} - (2N_x + 1)\right)$$

$$= \lim_{\eta \to 0} \frac{1}{4}[(2\eta)^{-2N_x} - (2N_x + 1)] = \frac{(2\eta)^{-2N_x}}{4}. \tag{41}$$

The wave functions [first part of Eq. (35)] now have the form

$$\begin{pmatrix} \psi_{A,\mathbf{i}} \\ \psi_{B,\mathbf{i}} \end{pmatrix} = \lim_{\eta \to 0} \frac{(-1)^n e^{i\left(\frac{\pi}{2} - \eta\right)m}}{\sqrt{N_y \cdot (2\eta)^{-2N_x}/4}} \begin{pmatrix} s \cdot \frac{1}{2} e^{(-\ln 2\eta)n} \\ \frac{1}{2} e^{(-\ln 2\eta)(N_x - n)} \end{pmatrix}$$

$$= \lim_{\eta \to 0} \frac{(-1)^n e^{i\frac{\pi}{2}m}}{\sqrt{N_y}} \begin{pmatrix} s \cdot (2\eta)^{N_x - n} \\ (2\eta)^n \end{pmatrix}. \tag{42}$$

From the last expression, we see that for the limit $\eta \to 0$ we have nonzero wave functions $\psi_{A,\mathbf{i}}$ only for $n = N_x$ (on the right zigzag edge) and nonzero wave functions $\psi_{B,\mathbf{i}}$ only for $n = 0$ (on the left one). So these wave functions in the limit can be written as entirely localized states:

$$\begin{pmatrix} \psi_{A,\mathbf{i}} \\ \psi_{B,\mathbf{i}} \end{pmatrix} = \frac{(-1)^n \cdot i^m}{\sqrt{N_y}} \begin{pmatrix} s \cdot \delta_{N_x,n} \\ \delta_{0,n} \end{pmatrix}, \tag{43}$$

where $\delta_{i,j}$ is the Kronecker delta.

It is important to note that we find two real wave functions in the case of even $N_x$. In the case of odd $N_x$, at the left edge wave functions are real; the right edge wave functions are imaginary. This can be changed by renormalization.

There are two basic entirely localized edge states depending on the parameter $s$ which describe the valence (conduction) band. They are illustrated in Fig. 6. However, because of their identical energies, one can construct a superposition of states and obtain a state entirely localized on only one zigzag edge (left or right).

Note that Eq. (43) does not depend on $N_x$. This means that these states have an identical form for all allowed values of

$N_x$ (even) and in the limit of the semi-infinite plane, a result which coincides with Ref. [19].

When we look at the right-hand limit $k_y = \frac{\pi}{2} + \eta$, where $\eta > 0$ (see Appendix B), we obtain a zero energy state with wave functions

$$\begin{pmatrix} \psi_{A,\mathbf{i}} \\ \psi_{B,\mathbf{i}} \end{pmatrix} = \frac{i^m}{\sqrt{N_y}} \begin{pmatrix} s \cdot \delta_{N_x,n} \\ \delta_{0,n} \end{pmatrix}. \tag{44}$$

This result differs by a factor of $(-1)^n$ compared to the left-hand limit [Eq. (43)]. In the case of even $N_x$, the resulting wave functions coincide. For odd $N_x$ they also coincide if one compares nonzero valence band wave functions (43) to nonzero conduction band wave functions (44) and vice versa. However, conduction and valence bands at the point $k_y = \pi/2$ have identical (zero) energy. Hence, wave functions in both forms [Eqs. (43) and (44)] are the same.

Note that this entirely localized state exists in the case of the carbon nanotube with open zigzag edges for $N_y$ divisible by 4. This can be seen from the allowed values of wave number $k_y$ [Eq. (22)].

### 4. Cases $k_y = k_y^c$, $\pi - k_y^c$

These values of wave number $k_y$ are on the borders between the case of all real roots and the case when one root of Eq. (20) is complex. All $N_x - 1$ real roots of Eq. (20) can be obtained numerically and the corresponding wave functions can be presented in the form of Eq. (27). The main interest is to describe wave functions and energies for the last root $k_x$, which tends to zero for $k_y \to \pi - k_y^c$ and tends to $\pi$ for $k_y$ approaching $k_y^c$. These points can be called transition points because here bulk states transform to edge states and vice versa.

First, let us look at the left transition point $k_y = k_y^c$. We start approaching this point from the left ($k_y = k_y^c - \eta$, $\eta \to 0^+$). The root of Eq. (20) that we are interested in tends to $\pi$ also from the left ($k_x = \pi - \lambda$, $\lambda > 0$).

We need to simplify the summation function (14). It is possible to do so by expanding into series formula (14) or substituting $k_x = \pi - \lambda$ at summation. We use the second approach:

$$S(k_x, N_x) = \lim_{\lambda \to 0} \sum_{n=1}^{N_x} \sin^2(\pi - \lambda)n = \sum_{n=1}^{N_x} (-1)^{2n} (\lambda n)^2$$

$$= \lambda^2 \sum_{n=1}^{N_x} n^2 = \lambda^2 \frac{N_x(N_x + 1)(2N_x + 1)}{6}. \tag{45}$$

Then, we need to simplify the sign function $s_1$ [Eq. (25)]:

$$s_1 = \lim_{\lambda \to 0} \text{sign}[\sin(\pi - \lambda)(N_x + 1)]$$

$$= \lim_{\lambda \to 0} \text{sign}[-(-1)^{N_x+1} \sin \lambda(N_x + 1)] = (-1)^{N_x}. \tag{46}$$

The next step is to calculate the function $\epsilon(k_x, k_y)$ [Eq. (29)], which is proportional to the energy $E_s$:

$$\epsilon(\pi, k_y^c)$$

$$= \lim_{\lambda, \eta \to 0} \sqrt{3 + 4\cos(\pi - \lambda)\cos(k_y^c - \eta) + 2\cos 2(k_y^c - \eta)}$$

$$= \sqrt{3 - 4\cos k_y^c + 2\cos 2k_y^c} = \frac{1}{N_x + 1}. \tag{47}$$

One can see that the energy $E_s = s \cdot t \cdot \epsilon(\pi, k_y^c)$ is different from zero, but approaches it in the case of the infinite (semi-infinite) system.

The last step is to simplify wave functions (27):

$$\begin{pmatrix} \psi_{A,\mathbf{i}} \\ \psi_{B,\mathbf{i}} \end{pmatrix} = \lim_{\lambda, \eta \to 0} \frac{e^{i(k_y^c - \eta)m}}{\sqrt{N_y \lambda} \sqrt{N_x(N_x + 1)(2N_x + 1)/6}}$$

$$\cdot \begin{pmatrix} (-1)^{N_x} s \sin[(\pi - \lambda)n] \\ \sin[(\pi - \lambda)(N_x - n)] \end{pmatrix}$$

$$= \frac{\sqrt{6} e^{ik_y^c m}}{\lambda \sqrt{N_y N_x(N_x+1)(2N_x+1)}} \begin{pmatrix} -s(-1)^{N_x+n} \lambda n \\ -(-1)^{N_x - n} \lambda(N_x - n) \end{pmatrix}$$

$$= \frac{(-1)^{N_x+n+1} \sqrt{6} e^{ik_y^c m}}{\sqrt{N_y N_x(N_x + 1)(2N_x + 1)}} \begin{pmatrix} s \cdot n \\ N_x - n \end{pmatrix}. \tag{48}$$

Here, at the last step we used the identity $(-1)^{-2n} = 1$. These wave functions can be renormalized to remove a factor $(-1)^{N_x+1}$. They also coincide with wave functions obtained from the right limit at the point after renormalization (for more details see Appendix C 1).

Another border point $k_y = \pi - k_y^c$ can be treated by analogy (see Appendices C 2 and C 3 for the left and the right limits, respectively). As a result, we have energies $E_s$ identical to the ones in the case $k_y = k_y^c$, and wave functions in the form

$$\begin{pmatrix} \psi_{A,\mathbf{i}} \\ \psi_{B,\mathbf{i}} \end{pmatrix} = \frac{(-1)^m \sqrt{6} e^{-ik_y^c m}}{\sqrt{N_y N_x(N_x + 1)(2N_x + 1)}} \begin{pmatrix} s \cdot n \\ N_x - n \end{pmatrix}. \tag{49}$$

Comparing the resulting wave functions for two transition points, $k_y = k_y^c$ [Eq. (48)] and $k_y = \pi - k_y^c$ [Eq. (49)], one can note their linear dependence on the horizontal index $n$, but in the first case there is an extra sign function that distinguishes between odd and even horizontal cells. In the second, there is a sign function which changes for different vertical positions of the cell $m$. Now we try to show that these sign functions work coherently: if one has value $+1$, the other one also equals $+1$, and vice versa for our choice of cell numeration. If one looks at Fig. 4 with our numeration convention, it is possible to note that for any cell, $n$ and $m$ are both odd or are both even. For shifted numeration one can get the opposite result: when $n$ is even $m$ is odd, and vice versa. For this case, the minus can be absorbed by renormalization. We could find only one work [11] where this transition point was considered, and the obtained result coincides with Eq. (49).

Note that obtained wave functions can be applied for both nanoribbons and nanotubes. The only difference is that for infinite nanoribbons the longitudinal wave number is continuous, and it is discrete for nanotubes.

## IV. FINITE SAMPLE

The easiest way to derive wave functions for a finite sample of rectangular geometry (Fig. 7) is to use the results of previous sections as a base. For the case of an armchair nanoribbon we found only one possible type of state (extended), but for zigzag nanoribbons we found a large variety of possible states. Therefore, we will use wave functions for zigzag nanoribbons which describe running waves in the $+y$ direction and superpose them with wave functions for zigzag nanoribbons
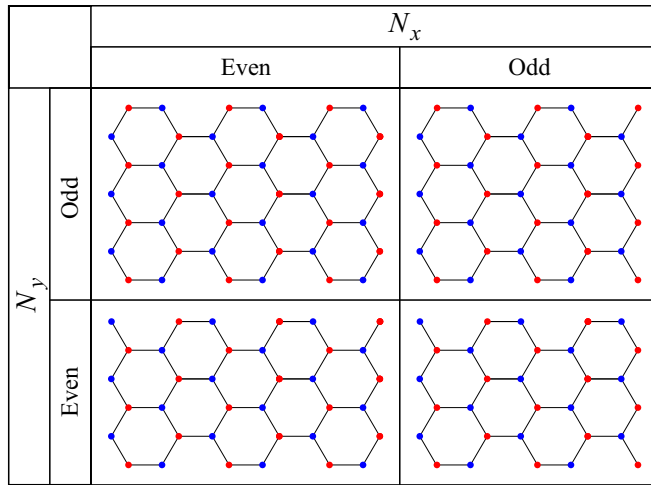
FIG. 7. Possible rectangular geometries of finite size honeycomb lattice.

which describe running waves in the $-y$ direction (obtained by changing $k_y$ to $-k_y$ in the formulas of Sec. III B). The resulting wave functions automatically satisfy the boundary conditions for zigzag nanoribbons [Eq. (19)], and after imposing boundary conditions for armchair nanoribbons [Eq. (9)], terms $e^{ik_y m}$ transform to $\sin k_y m$ as in Sec. III A. Normalization constants should also be changed: instead of factors $1/\sqrt{N_y}$, there should be $1/\sqrt{S(k_y, N_y)}$.

The eigenvalue problem (4) for a finite sample with $N_x \times N_y$ sites should have $N_x \times N_y$ eigenvalues and eigenvectors. If we take all possible values $k_y$ [Eq. (10)] from the armchair nanoribbon solution and solve the transcendental Eq. (20) for each of them, finally we get $2N_x N_y$ solutions. Here the doubling comes from valence and conduction band solutions. The solution to this problem is as follows: Pairs of wave numbers $(k_x, k_y)$ and $(\pi - k_x, \pi - k_y)$ describe identical states (see Appendix D for the proof). Therefore, we can halve the number of such pairs, considering that [12]

$$k_y = \frac{\pi j_y}{N_y + 1}, \quad j_y = 1, 2, 3, \ldots, \frac{N_y + 1}{2} \quad \left(0 < k_y \leqslant \frac{\pi}{2}\right) \tag{50}$$

and

$$0 < k_x < \pi \quad \left(0 < k_y < \frac{\pi}{2}\right), \tag{51}$$

$$0 < k_x \leqslant \frac{\pi}{2} \quad \left(k_y = \frac{\pi}{2}\right), \tag{52}$$

which are to be found from Eq. (20).

Note that the entirely localized states which were found in zigzag nanoribbons for $k_y = \pi/2$ in Sec. III B 3 also exist in finite honeycomb systems. However, the special value of wave number $k_y = \pi/2$ cannot be obtained for systems with even $N_y$ [see Eq. (50) and forbidden geometries in the second line of Fig. 7].

We divide further explanations into subsections, where we find wave functions for different regions (points) of wave number $k_y$.

### 1. Case $k_y \in (0; k_y^c)$

All solutions in this region of $k_y$ correspond to extended states. Energies can be calculated by formulas (6). Wave functions for zigzag nanoribbon [Eq. (27)] are modified to

$$\begin{pmatrix} \psi_{A,\mathbf{i}} \\ \psi_{B,\mathbf{i}} \end{pmatrix} = \frac{\sin k_y m}{\sqrt{S(k_x, N_x) S(k_y, N_y)}} \begin{pmatrix} s_1 s \sin(k_x n) \\ \sin[k_x(N_x - n)] \end{pmatrix}, \tag{53}$$

where the sign function $s_1$ is still defined by Eq. (25). The possible $N_x$ real values of wave number $k_x$ for each $k_y$ can be found numerically from Eq. (20).

This result is identical to the wave functions obtained in Ref. [12]. If one wants to compare this result to wave functions obtained for a unit cell consisting of four atoms [13,17], they need to know that in that case the Brillouin zone is smaller. This leads to the appearance of additional dispersion branches which are artificially made by introducing a factor $\pm 1$ in the second term of $\epsilon(k_x, k_y)$ [Eq. (6)] (the second branch appears for $k_x \to \pi + k_x$ in our notation). This is the reason why direct comparison of our result to the results in Refs. [13,17] is difficult. We note that their wave functions coincide with our result [Eq. (53)] if we do not take into account the factor which describes additional branches.

There are $N_x - 1$ real roots of the transcendental Eq. (20), with corresponding extended states described by wave functions (53) for the region of $k_y \in [k_y^c; \pi/2)$. Next, we discuss the only complex root of Eq. (20) and the corresponding wave functions in the above-mentioned region for wave number $k_y$. We will talk later about the point $k_y = \pi/2$ and discuss both real and complex roots.

### 2. Case $k_y \in (k_y^c; \pi/2)$

We obtain these wave functions by modifying wave functions for zigzag nanoribbons [Eq. (35)] for the region $k_y \in (k_y^c; \pi/2)$:

$$\begin{pmatrix} \psi_{A,\mathbf{i}} \\ \psi_{B,\mathbf{i}} \end{pmatrix} = \frac{(-1)^n \sin k_y m}{\sqrt{S_{\text{hyp}}(k_x', N_x) S(k_y, N_y)}} \begin{pmatrix} s \sinh(k_x' n) \\ \sinh[k_x'(N_x - n)] \end{pmatrix}, \tag{54}$$

where $k_x'$ is a positive root of the following equation:

$$\sinh k_x' N_x - 2 \cos k_y \sinh[k_x'(N_x + 1)] = 0. \tag{55}$$

The same result can be derived directly from wave functions (53) with the complex plane continuation $k_x = \pi + ik_x'$ by analogy with the calculation in Appendix A. Corresponding energies have the form

$$E_s = s \cdot t \sqrt{3 - 4 \cosh k_x' \cos k_y + 2 \cos 2k_y}. \tag{56}$$

The result [Eq. (54)] agrees with the recent work [12] that explored localized states in finite systems with rectangular geometry.

### 3. Case $k_y = k_y^c$

In this case $k_x$ tends to $\pi$. We can use wave functions (48) or (49) as a basis, where we need to change $e^{ik_y^c m}$ (or $e^{-ik_y^c m}$) to $\sin k_y^c m$ together with changing the normalization coefficient.

We rewrite Eq. (48) as

$$\begin{pmatrix} \psi_{A,\mathbf{i}} \\ \psi_{B,\mathbf{i}} \end{pmatrix} = \frac{(-1)^{N_x+n+1}\sqrt{6}\sin k_y^c m}{\sqrt{N_x(N_x+1)(2N_x+1)S(k_y^c, N_y)}} \begin{pmatrix} s \cdot n \\ N_x - n \end{pmatrix}.$$

(57)

One can obtain this result as a left-hand limit to the point $k_y = k_y^c$ for finite sample extended wave functions (53) or a right-hand limit of localized wave functions (54). If one wants to check coincidence of wave functions after replacement $(k_x, k_y) \rightarrow (\pi - k_x, \pi - k_y)$, a straightforward approach here cannot be done. In this case, we need to look at the right-hand limit of wave functions (53) at the point $k_y = \pi - k_y^c$, which is treated as in Appendix C 3, and we come to the result

$$\begin{pmatrix} \psi_{A,\mathbf{i}} \\ \psi_{B,\mathbf{i}} \end{pmatrix} = \frac{(-1)^{m+1}\sqrt{6}\sin k_y^c m}{\sqrt{N_x(N_x+1)(2N_x+1)S(k_y^c, N_y)}} \begin{pmatrix} s \cdot n \\ N_x - n \end{pmatrix}.$$

(58)

The explanation for why factor $(-1)^m$ in Eq. (57) is the same as $(-1)^n$ in Eq. (58) was shown at the end of Sec. III B.

Corresponding energies coincide with energies found for zigzag nanoribbons in the case $k_y = k_y^c$:

$$E_s = \frac{s \cdot t}{N_x + 1}.$$

(59)

#### 4. Case $k_y = \pi/2$

This case is only possible for odd $N_y$ [as $k_y$ values have the form of Eq. (50)]. We start by describing a sample with odd $N_x$ and $N_y$. Possible $k_x$ values can be found analytically from Eq. (36) by taking into account the constraints of Eq. (52):

$$k_x = \frac{\pi}{N_x} j_x, \quad j_x = 1, 2, 3, \ldots, \frac{N_x - 1}{2}.$$

(60)

The corresponding extended wave functions are described by formulas (53).

Now let us count the number of roots of the eigenvalue problem (4) for a rectangular system with $N_x N_y$ sites. For $k_y \in (0; \frac{\pi}{2})$ there are $N_x(N_y - \frac{1}{2})$ solutions, and for $k_y = \frac{\pi}{2}$ and $k_x \in (0; \frac{\pi}{2})$ we have $N_x - 1$ solutions (doubling comes from the two possible bands). So there is only one root remaining that we need to find. We expect to find it as a limit of a complex one like we found for the entirely localized state in Sec. III B for $k_y = \pi/2$. Considering the left-hand limit $k_y = \frac{\pi}{2} - \eta$ (where $\eta \rightarrow 0^+$), one can obtain by analogy with Sec. III B $k_x = \pi \pm i k_x'$ ($k_x'$ tends to infinity). This state has zero energy [see Eq. (40)], and the corresponding wave function can be written using the Kronecker delta function:

$$\begin{pmatrix} \psi_{A,\mathbf{i}} \\ \psi_{B,\mathbf{i}} \end{pmatrix} = \frac{(-1)^n \cdot \sin \frac{\pi}{2} m}{\sqrt{N_y}} \begin{pmatrix} s \cdot \delta_{N_x,n} \\ \delta_{0,n} \end{pmatrix}.$$

(61)

However, this result can be significantly simplified. When one looks at our numeration convention (Fig. 4) and geometry of the system we study now (odd $N_x$ and $N_y$, upper right corner of Fig. 7) they can note that the wave function at $B$ sites is zero. It comes from the factor $\delta_{0,n} \sin \frac{\pi}{2} m$. The first function is nonzero only for $n = 0$ (left edge), but at the left edge $m$ is even and $\sin \frac{\pi}{2} m = 0$. Finally, the wave function can be
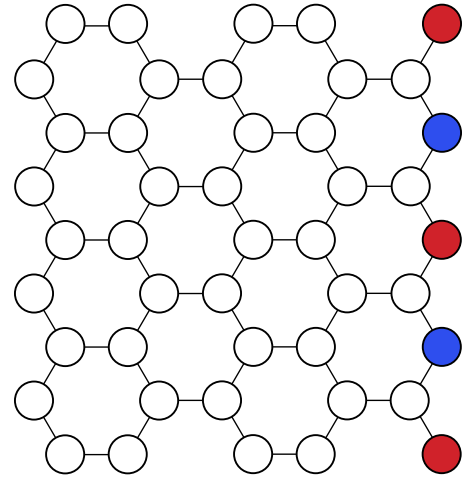


FIG. 8. Wave function for the entirely localized state in a finite honeycomb system [Eq. (62)]. The amplitudes are normalized by the maximum value of the respective wave functions. Here blue, white, and red correspond to amplitudes $-1$, 0, and 1, respectively.

written as

$$\begin{pmatrix} \psi_{A,\mathbf{i}} \\ \psi_{B,\mathbf{i}} \end{pmatrix} = \frac{\delta_{N_x,n} \sin \frac{\pi}{2} m}{\sqrt{(N_y+1)/2}} \begin{pmatrix} 1 \\ 0 \end{pmatrix},$$

(62)

where we have removed the factor $(-1)^n$ because it was multiplied by a function which is nonzero at the right edge ($n = N_x = \text{const}$) and changed the normalization constant, because the previous one was derived assuming that the wave function is localized on both left and right edges, but for this geometry it can be localized only on the right edge. Here the band index $s$ is also absent because it is easy to show that after renormalization wave functions both conductance and valence bands are identical. Therefore, we have found the last solution of the eigenvalue problem (4) in the case of odd $N_x$. This wave function is illustrated in Fig. 8.

Such rectangular geometry (odd $N_x$ and $N_y$) was studied numerically [12] and this entirely localized state was also observed.

We now switch to the case of even $N_x$ and odd $N_y$. Possible $k_x$ values are as follows:

$$k_x = \frac{\pi}{N_x} j_x, \quad j_x = 1, 2, 3, \ldots, \frac{N_x}{2}.$$

(63)

The corresponding wave functions (53) describe extended states. There is an exception for normalization coefficient in Eq. (53) at the point $k_x = k_y = \frac{\pi}{2}$ it should be equal to $(\frac{1}{2}N_x(N_y+1))^{-1/2}$.

If one counts the number of roots like we did earlier, they will find that we already have the correct amount of solutions for problem (4). Consequently, there are no entirely localized states for rectangular geometry with even $N_x$ and odd $N_y$ (upper left corner of Fig. 7). Let us also show it based on the result [Eq. (61)]: One can see that both Kronecker delta functions are nonzero for either $n = 0$ or $n = N_x$ (which is even), on both these edges $m$ is even and $\sin \frac{\pi}{2} m = 0$ [because of our indexation convention (Fig. 4)], and we have zero wave function everywhere. This is nonphysical, and we can say that a zero energy state for this geometry is not realizable.

All obtained solutions are numerically verified to satisfy Schrödinger Eq. (4) and both normalization conditions [Eq. (12)].

## V. DISCUSSION

Electronic properties of boundaries of the honeycomb lattice are one of the most basic problems of systems with boundaries, physically realized in graphene, artificial honeycomb structures, and ultracold atoms in honeycomb optical lattices. The most studied example of a boundary is the semi-infinite graphene sheet with a zigzag edge [9,18,19,28]. It was shown that this has a band of zero-energy surface states for $k_y \in (\frac{1}{3}\pi; \frac{2}{3}\pi)$ in our notation, with dimensionless penetration length given by $\lambda = -1/\ln |2\cos k_y|$. For this system, it was also shown that there exists a state with an entirely localized wave function at the edge for $k_y = \pi/2$ (similar to the states we found for zigzag nanoribbons and nanotubes in Fig. 6 and rectangular graphene nanoflake in Fig. 8). For zigzag nanoribbons, these authors discussed edge states with $E \approx 0$ [18], but a state with zero energy was not mentioned.

A zero energy state was numerically studied for finite graphene nanoflakes [12] and the state illustrated in Fig. 8 was found. The reason for its appearance is thought to be sublattice imbalance (number of sites of $A$ and $B$ sublattices differs by 1). It was also noted that this state cannot be described by the usual extended or localized wave function representations. However, we showed that entirely localized states should be treated as a limit of localized states when $k_y \to \pi/2$ and $E \to 0$ and clarified possible rectangular geometries for their existence.

The presence of boundaries completely modifies the energy dispersion diagram of infinite graphene sheet (Figs. 3 and 5). In the same manner, localized states change optical properties of the material [11]. Taking into account entirely localized states that we found should affect positions and amplitudes of the optical adsorption spectra. Transport [20] and electromagnetic [21] properties are also altered after taking into consideration the edge states. For the zigzag nanoribbon valence and conduction band, touching is located at the point $k_y = \frac{\pi}{2}$, where we found entirely localized states, so the point has double exceptionality: zero energy and band touching. Our paper discusses an analytical treatment of the point. We showed that entirely localized states with zero energy (when the wave function is nonzero only at the edge sites) exist in zigzag nanoribbons, zigzag nanotubes with number of sites along the zigzag edge divisible by 4, and rectangular graphene nanoflakes with an odd number of sites along the zigzag and armchair edges.

We also described the transition point between extended and localized states. Here wave functions can be written as linear functions of the horizontal index $n$ times the sign changing function $(-1)^n$. It looks like a localized state with critical (i.e., infinite) penetration length.

After this work was completed, we became aware of the recent studies of graphene ribbons [29].

## ACKNOWLEDGMENTS

## APPENDIX A: DERIVATION OF WAVE FUNCTIONS FOR LOCALIZED CASE

First, let us derive wave functions for the case of complex plane continuation in the form $k_x = \pi + ik'_x$, where $k'_x > 0$. We start from simplifying the sign function $s_1$ [Eq. (25)] using the identity $\sin(\pi + ik'_x)n = i(-1)^n \sinh k'_x n$:

$$
\begin{aligned}
s_1 &= \frac{\sqrt{\sin^2(\pi + ik'_x)}}{\sin(\pi + ik'_x)} \cdot \frac{\sin[(\pi + ik'_x)(N_x + 1)]}{\sqrt{\sin^2[(\pi + ik'_x)(N_x + 1)]}} \\
&= \frac{\sqrt{(-i\sinh k'_x)^2}}{-i\sinh k'_x} \cdot \frac{i(-1)^{N_x+1}\sinh k'_x(N_x + 1)}{\sqrt{[i(-1)^{N_x+1}\sinh k'_x(N_x + 1)]^2}} \\
&= (-1)^{N_x}.
\end{aligned} \tag{A1}
$$

Now we can rewrite the wave functions from Eq. (24):

$$
\begin{aligned}
\begin{pmatrix} \psi_{A,\mathbf{i}} \\ \psi_{B,\mathbf{i}} \end{pmatrix} &= -\sqrt{2}ic'_3 e^{i[(\pi + ik'_x)N_x + k_y m]} \\
&\quad \cdot \begin{pmatrix} (-1)^{N_x} s \sin[(\pi + ik'_x)n] \\ \sin[(\pi + ik'_x)(N_x - n)] \end{pmatrix} \\
&= (-1)^{N_x+1}\sqrt{2}ic'_3 e^{-k'_x N_x + ik_y m} \\
&\quad \cdot \begin{pmatrix} (-1)^{N_x} s \cdot i(-1)^n \sinh k'_x n \\ i(-1)^{N_x - n}\sinh k'_x(N_x - n) \end{pmatrix} \\
&= (-1)^{n+2}\sqrt{2}c'_3 e^{-k'_x N_x + ik_y m} \\
&\quad \cdot \begin{pmatrix} s(-1)^{2N_x}\sinh k'_x n \\ (-1)^{2N_x - 2n}\sinh k'_x(N_x - n) \end{pmatrix} \\
&= (-1)^n \sqrt{2}c'_3 e^{-k'_x N_x + ik_y m} \begin{pmatrix} s\sinh k'_x n \\ \sinh k'_x(N_x - n) \end{pmatrix}. \tag{A2}
\end{aligned}
$$

In the second possible case of continuation ($k_x = 0 + ik'_x$, where $k'_x > 0$) we apply the identity $\sin ik'_x n = i\sinh k'_x n$. First, we rewrite $s_1$ as

$$
\begin{aligned}
s_1 &= \frac{\sqrt{\sin^2(ik'_x)}}{\sin(ik'_x)} \cdot \frac{\sin[ik'_x(N_x + 1)]}{\sqrt{\sin^2[ik'_x(N_x + 1)]}} \\
&= \frac{\sqrt{(i\sinh k'_x)^2}}{i\sinh k'_x} \cdot \frac{i\sinh k'_x(N_x + 1)}{\sqrt{[i\sinh k'_x(N_x + 1)]^2}} = 1. \tag{A3}
\end{aligned}
$$

The next step is to present wave functions (24) in the following form:

$$
\begin{aligned}
\begin{pmatrix} \psi_{A,\mathbf{i}} \\ \psi_{B,\mathbf{i}} \end{pmatrix} &= -\sqrt{2}ic'_3 e^{i(ik'_x N_x + k_y m)} \begin{pmatrix} 1 \cdot s \sin(ik'_x n) \\ \sin[ik'_x(N_x - n)] \end{pmatrix} \\
&= -\sqrt{2}ic'_3 e^{-k'_x N_x + ik_y m} \begin{pmatrix} s \cdot i\sinh k'_x n \\ i\sinh k'_x(N_x - n) \end{pmatrix} \\
&= \sqrt{2}c'_3 e^{-k'_x N_x + ik_y m} \begin{pmatrix} s\sinh k'_x n \\ \sinh k'_x(N_x - n) \end{pmatrix}. \tag{A4}
\end{aligned}
$$

Here we used a non- normalized expression for extended wave functions [Eq. (24)] instead of a normalized one [Eq. (27)] in order not to transform summation formula (14), because we need to renormalize the resulting wave functions.

## APPENDIX B: RIGHT LIMIT OF WAVE FUNCTIONS AND ENERGIES FOR ZIGZAG NANORIBBONS IN THE CASE $k_y = \pi/2$

For this type of limit we present wave number $k_y$ as $\frac{\pi}{2} + \eta$, where $\eta \to 0^+$. Acting by analogy with Sec. III B 3, we can write that wave number $k_x$ has the form $0 \pm ik'_x$, where $k'_x$ tends to infinity. The eigenvalue equation [second part of Eq. (30)] in these limits can be written as

$$\frac{1}{2} e^{k'_x N_x} + 2 \cos\left(\frac{\pi}{2} + \eta\right) \cdot \frac{1}{2} e^{k'_x (N_x + 1)} = 0, \quad \text{(B1)}$$

with solution

$$k'_x = -\ln 2\eta. \quad \text{(B2)}$$

This dependence $k'_x$ on $\eta$ is identical in the left-hand limit.

Eigenenergies $E_s$ tend to zero, because the function $\epsilon(k'_x, \frac{\pi}{2})$ [Eq. (29)] tends to zero:

$$\epsilon\left(k'_x, \frac{\pi}{2}\right) = \sqrt{3 + 4 \cdot \frac{1}{2} e^{k'_x} \cos k_y + 2 \cos 2 k_y}$$

$$= \lim_{\eta \to 0} \sqrt{3 + 2 e^{-\ln 2\eta} \cos\left(\frac{\pi}{2} + \eta\right) + 2 \cos 2\left(\frac{\pi}{2} + \eta\right)}$$

$$= \lim_{\eta \to 0} \sqrt{3 - 2 \cdot (2\eta)^{-1} \eta + 2 \cdot (-1)} = 0. \quad \text{(B3)}$$

The summation function (34) inside wave functions (35) simplifies. It has a form identical to Eq. (41). Finally, the wave functions [second part of Eq. (35)] become

$$\begin{pmatrix} \psi_{A,\mathbf{i}} \\ \psi_{B,\mathbf{i}} \end{pmatrix} = \lim_{\eta \to 0} \frac{e^{i\left(\frac{\pi}{2} + \eta\right)m}}{\sqrt{N_y \cdot (2\eta)^{-2N_x}/4}} \begin{pmatrix} s \cdot \frac{1}{2} e^{(-\ln 2\eta)n} \\ \frac{1}{2} e^{(-\ln 2\eta)(N_x - n)} \end{pmatrix}$$

$$= \lim_{\eta \to 0} \frac{e^{i\frac{\pi}{2}m}}{\sqrt{N_y}} \begin{pmatrix} s \cdot (2\eta)^{N_x - n} \\ (2\eta)^n \end{pmatrix}. \quad \text{(B4)}$$

Similarly to Eqs. (42) and (43), we can rewrite the result from Eq. (B4) using Kronecker delta functions:

$$\begin{pmatrix} \psi_{A,\mathbf{i}} \\ \psi_{B,\mathbf{i}} \end{pmatrix} = \frac{i^m}{\sqrt{N_y}} \begin{pmatrix} s \cdot \delta_{N_x, n} \\ \delta_{0, n} \end{pmatrix}. \quad \text{(B5)}$$

## APPENDIX C: SIMPLIFICATION OF WAVE FUNCTIONS FOR ZIGZAG NANORIBBONS IN CASES $k_y = k_y^c$, $\pi - k_y^c$

Here we provide the rest of the limits of wave functions at transition points $k_y = k_y^c$, $\pi - k_y^c$ that are not mentioned in the main text.

### 1. Right limit of wave functions at the point $k_y = k_y^c$

We are interested in results for complex plane continuation of type $k_x = \pi \pm ik'_x$. We represent wave number $k_y$ in the form $k_y^c + \eta$, where $\eta \to 0^+$. In this limit, $k'_x$ also tends to zero. Let us start from simplification summation function

(34):

$$S_{\text{hyp}}(k'_x, N_x) = \lim_{k'_x \to 0} \frac{1}{4}\left(\frac{\sinh k'_x (2N_x + 1)}{\sinh k'_x} - (2N_x + 1)\right)$$

$$= \frac{1}{6} N_x (N_x + 1)(2N_x + 1)(k'_x)^2. \quad \text{(C1)}$$

The wave functions [first part of Eq. (35)] can be written as

$$\begin{pmatrix} \psi_{A,\mathbf{i}} \\ \psi_{B,\mathbf{i}} \end{pmatrix} = \lim_{\eta, k'_x \to 0} \frac{(-1)^n e^{i(k_y^c + \eta)m}}{\sqrt{N_y} k'_x \sqrt{N_x(N_x + 1)(2N_x + 1)/6}}$$

$$\cdot \begin{pmatrix} s k'_x n \\ k'_x (N_x - n) \end{pmatrix}$$

$$= \frac{(-1)^n \sqrt{6} e^{ik_y^c m}}{\sqrt{N_y N_x (N_x + 1)(2N_x + 1)}} \begin{pmatrix} s \cdot n \\ N_x - n \end{pmatrix}. \quad \text{(C2)}$$

This wave functions differ from Eq. (48) by the factor $(-1)^{N_x + 1}$, but it can be easily absorbed by renormalization. The energy related function $\epsilon(k_x, k_y)$ for this case has the same values as in Eq. (47).

### 2. Left limit of wave functions at the point $k_y = \pi - k_y^c$

We need to use complex plane continuation of the form $k_x = 0 \pm ik'_x$, for the left limit $k_y = \pi - k_y^c - \eta$ ($\eta \to 0^+$) leads to limiting to zero of $k'_x$. Summation function (34) will have the form of Eq. (C1), so the wave functions [second part of Eq. (35)] can be simplified as follows:

$$\begin{pmatrix} \psi_{A,\mathbf{i}} \\ \psi_{B,\mathbf{i}} \end{pmatrix} = \lim_{\eta, k'_x \to 0} \frac{e^{i(\pi - k_y^c - \eta)m}}{\sqrt{N_y} k'_x \sqrt{N_x(N_x + 1)(2N_x + 1)/6}}$$

$$\cdot \begin{pmatrix} s k'_x n \\ k'_x (N_x - n) \end{pmatrix}$$

$$= \frac{(-1)^m \sqrt{6} e^{-ik_y^c m}}{\sqrt{N_y N_x (N_x + 1)(2N_x + 1)}} \begin{pmatrix} s \cdot n \\ N_x - n \end{pmatrix}. \quad \text{(C3)}$$

Let us calculate the function $\epsilon(k_x, k_y)$ [second part of Eq. (29)]:

$$\epsilon\left(0, \pi - k_y^c\right) = \lim_{\eta, k'_x \to 0} \left[3 + 4 \cosh k'_x \cos\left(\pi - k_y^c - \eta\right)\right.$$

$$\left. + 2 \cos 2\left(\pi - k_y^c - \eta\right)\right]^{1/2}$$

$$= \sqrt{3 - 4 \cos k_y^c + 2 \cos 2k_y^c} = \frac{1}{N_x + 1}, \quad \text{(C4)}$$

which is identical to the value of this function at another transition point $k_y = k_y^c$ [Eq. (47)].

### 3. Right limit of wave functions at the point $k_y = \pi - k_y^c$

We have extended states [Eq. (27)] in the region $k_y = \pi - k_y^c + \eta$ ($\eta > 0$). The wave number $k_x$ tends to zero when $\eta \to 0$. The summation function (14) in this case can be calculated similarly to Eq. (45):

$$S(k_x, N_x) = \lim_{k_x \to 0} \sum_{n=1}^{N_x} \sin^2 k_x n = k_x^2 \sum_{n=1}^{N_x} n^2$$

$$= k_x^2 \frac{N_x (N_x + 1)(2N_x + 1)}{6}. \quad \text{(C5)}$$

The sign function $s_1$ [Eq. (25)] also transforms:

$$s_1 = \lim_{k_x \to 0} \text{sign}(\sin k_x(N_x + 1)) = 1. \qquad \text{(C6)}$$

Finally, we can write simplified wave functions:

$$\begin{pmatrix} \psi_{A,\mathbf{i}} \\ \psi_{B,\mathbf{i}} \end{pmatrix} = \lim_{\eta, k_x \to 0} \frac{e^{i(\pi - k_y^c + \eta)m}}{\sqrt{N_y k_x} \sqrt{N_x(N_x + 1)(2N_x + 1)/6}}$$

$$\cdot \begin{pmatrix} s k_x n \\ k_x(N_x - n) \end{pmatrix}$$

$$= \frac{(-1)^m \sqrt{6} e^{-ik_y^c m}}{\sqrt{N_y N_x(N_x + 1)(2N_x + 1)}} \begin{pmatrix} s \cdot n \\ N_x - n \end{pmatrix}. \qquad \text{(C7)}$$

This result coincides with the left limit at the point $k_y = \pi - k_y^c$ [Eq. (C3)]. The function $\epsilon(k_x, k_y)$ at this point has the value of Eq. (C4).

In all considered cases, left and right limits give identical (up to renormalization) wave functions and coinciding energies. This result is in accordance with the principle of continuity.

## APPENDIX D: PROOF THAT PAIRS $(k_x, k_y)$ AND $(\pi - k_x, \pi - k_y)$ DESCRIBE IDENTICAL STATES

### 1. Extended states

We start from proving that the function $\epsilon(k_x, k_y)$ has the same values for these pairs of $(k_x, k_y)$:

$$\epsilon(\pi - k_x, \pi - k_y)$$

$$= \sqrt{3 + 4 \cos(\pi - k_x) \cos(\pi - k_y) + 2 \cos 2(\pi - k_y)}$$

$$= \sqrt{3 + 4 \cos k_x \cos k_y + 2 \cos 2k_y} = \epsilon(k_x, k_y). \qquad \text{(D1)}$$

This means that these states also have identical energies.

Now let us do the same thing for wave functions (53). First, we study what happens to the sign function $s_1$ [Eq. (25)] which depends only on $k_x$:

$$s_1(\pi - k_x) = \text{sign}\{\sin[(\pi - k_x)(N_x + 1)]\}$$

$$= \text{sign}\{-(-1)^{N_x+1} \sin[k_x(N_x + 1)]\}$$

$$= (-1)^{N_x} \text{sign}\{\sin[k_x(N_x + 1)]\}$$

$$= (-1)^{N_x} s_1(k_x). \qquad \text{(D2)}$$

The summation function $S(k, N)$ also does not change for $k \to \pi - k$. The second step is to rewrite wave functions (53):

$$\begin{pmatrix} \psi_{A,\mathbf{i}} \\ \psi_{B,\mathbf{i}} \end{pmatrix} = \frac{\sin(\pi - k_y)m}{\sqrt{S(k_x, N_x) S(k_y, N_y)}}$$

$$\cdot \begin{pmatrix} (-1)^{N_x} s_1(k_x) s \sin[(\pi - k_x)n] \\ \sin[(\pi - k_x)(N_x - n)] \end{pmatrix}$$

$$= \frac{(-1)^{m+1} \sin k_y m}{\sqrt{S(k_x, N_x) S(k_y, N_y)}}$$

$$\times \begin{pmatrix} (-1)^{N_x+n+1} s_1(k_x) s \sin(k_x n) \\ (-1)^{N_x-n+1} \sin[k_x(N_x - n)] \end{pmatrix}$$

$$= \frac{(-1)^{N_x+m+n} \sin k_y m}{\sqrt{S(k_x, N_x) S(k_y, N_y)}} \begin{pmatrix} s_1(k_x) s \sin(k_x n) \\ (-1)^{-2n} \sin[k_x(N_x - n)] \end{pmatrix}. \qquad \text{(D3)}$$

These wave functions coincide with wave functions for $(k_x, k_y)$ [Eq. (53)], because $(-1)^{2n} = 1$ and $(-1)^{m+n}$ are constant for all sites (it depends on cell numeration choice: in our case of numeration as in Fig. 2, it is always $+1$), and finally $(-1)^{N_x}$ can be absorbed by renormalization.

### 2. Localized states

For the region $k_y \in (k_y^c; \pi/2)$ wave functions and eigenenergies have the form of Eqs. (54) and (56), respectively. If one wants to make the change $(k_x, k_y) \to (\pi - k_x, \pi - k_y)$ they need to know the wave functions and energies for the region $k_y \in (\pi/2; \pi - k_y^c)$. We derive wave functions and eigenenergies for $k_y \in (\pi/2; \pi - k_y^c)$ from wave functions [second part of Eq. (35)] and eigenenergies [second part of Eq. (29)] for zigzag nanoribbons:

$$\begin{pmatrix} \psi_{A,\mathbf{i}} \\ \psi_{B,\mathbf{i}} \end{pmatrix} = \frac{\sin k_y m}{\sqrt{S_{\text{hyp}}(k_x', N_x) S(k_y, N_y)}} \begin{pmatrix} s \sinh(k_x' n) \\ \sinh[k_x'(N_x - n)] \end{pmatrix}, \qquad \text{(D4)}$$

$$E_s = s \cdot t \sqrt{3 + 4 \cosh k_x' \cos k_y + 2 \cos 2k_y}. \qquad \text{(D5)}$$

Now, we make the replacement $(k_x, k_y) \to (\pi - k_x, \pi - k_y)$ in Eqs. (D4) and (D5) to compare these results with Eqs. (54) and (56), respectively.

Let us start by comparing energies. The parameter $k_x'$ does not change because the change $k_x \to \pi - k_x$ is already included in different types of complex plane continuations [Eq. (28)]. So, we only need to change $k_y \to \pi - k_y$ in Eq. (D5):

$$E_s = s \cdot t \sqrt{3 + 4 \cosh k_x' \cos(\pi - k_y) + 2 \cos 2(\pi - k_y)}$$

$$= s \cdot t \sqrt{3 - 4 \cosh k_x' \cos k_y + 2 \cos 2k_y}, \qquad \text{(D6)}$$

which coincides with the energy in Eq. (56).

Now we compare wave functions in the same way — we exchange only $k_y \to \pi - k_y$ (summation functions remain the same):

$$\begin{pmatrix} \psi_{A,\mathbf{i}} \\ \psi_{B,\mathbf{i}} \end{pmatrix} = \frac{\sin(\pi - k_y)m}{\sqrt{S_{\text{hyp}}(k_x', N_x) S(k_y, N_y)}} \begin{pmatrix} s \sinh(k_x' n) \\ \sinh[k_x'(N_x - n)] \end{pmatrix}$$

$$= \frac{(-1)^{m+1} \sin k_y m}{\sqrt{S_{\text{hyp}}(k_x', N_x) S(k_y, N_y)}} \begin{pmatrix} s \sinh(k_x' n) \\ \sinh[k_x'(N_x - n)] \end{pmatrix}. \qquad \text{(D7)}$$

This result is identical to wave functions (54), because factors $(-1)^m$ in Eq. (D7) and $(-1)^n$ in Eq. (54) work the same way (explained at the end of Sec. III B) and $(-1)$ can be absorbed by renormalization.

[1] J. Cai, P. Ruffieux, R. Jaafar, M. Bieri, T. Braun, S. Blankenburg, M. Muoth, A. P. Seitsonen, M. Saleh, X. Feng *et al.*, Atomically precise bottom-up fabrication of graphene nanoribbons, Nature (London) **466**, 470 (2010).

[2] A. H. Castro Neto, F. Guinea, N. M. R. Peres, K. S. Novoselov, and A. K. Geim, The electronic properties of graphene, Rev. Mod. Phys. **81**, 109 (2009).

[3] Y. Kobayashi, K.-I. Fukui, T. Enoki, K. Kusakabe, and Y. Kaburagi, Observation of zigzag and armchair edges of graphite using scanning tunneling microscopy and spectroscopy, Phys. Rev. B **71**, 193406 (2005).

[4] Y. Kobayashi, K.-I. Fukui, T. Enoki, and K. Kusakabe, Edge state on hydrogen-terminated graphite edges investigated by scanning tunneling microscopy, Phys. Rev. B **73**, 125415 (2006).

[5] C. Tao, L. Jiao, O. V. Yazyev, Y.-C. Chen, J. Feng, X. Zhang, R. B. Capaz, J. M. Tour, A. Zettl, S. G. Louie *et al.*, Spatially resolving edge states of chiral graphene nanoribbons, Nat. Phys. **7**, 616 (2011).

[6] P. R. Wallace, The band theory of graphite, Phys. Rev. **71**, 622 (1947).

[7] K. Wakabayashi and S. Dutta, Nanoscale and edge effect on electronic properties of graphene, Solid State Commun. **152**, 1420 (2012).

[8] K. Wakabayashi, K.-I. Sasaki, T. Nakanishi, and T. Enoki, Electronic states of graphene nanoribbons and analytical solutions, Sci. Tech. Adv. Mater. **11**, 054504 (2010).

[9] K. Wakabayashi, M. Fujita, H. Ajiki, and M. Sigrist, Electronic and magnetic properties of nanographite ribbons, Phys. Rev. B **59**, 8271 (1999).

[10] M. Moradinasab, H. Nematian, M. Pourfath, M. Fathipour, and H. Kosina, Analytical models of approximations for wave functions and energy dispersion in zigzag graphene nanoribbons, J. Appl. Phys. **111**, 074318 (2012).

[11] V. A. Saroka, M. V. Shuba, and M. E. Portnoi, Optical selection rules of zigzag graphene nanoribbons, Phys. Rev. B **95**, 155438 (2017).

[12] H. Yorikawa, Edge states and sublattice imbalance of rectangular graphene nanoflakes, J. Phys. Commun. **5**, 055007 (2021).

[13] L. Malysheva and A. Onipko, Spectrum of $\pi$ Electrons in Graphene as a Macromolecule, Phys. Rev. Lett. **100**, 186806 (2008).

[14] L. Malysheva, Spectral problem for graphene fragments and polyenes: An analytic approach, Phys. Status Solidi B **254**, 1600773 (2017).

[15] A. Onipko and L. Malysheva, Electron spectrum of graphene macromolecule revisited, Phys. Status Solidi B **255**, 1700248 (2018).

[16] A. Onipko, Spectrum of $\pi$ electrons in graphene as an alternant macromolecule and its specific features in quantum conductance, Phys. Rev. B **78**, 245412 (2008).

[17] J. Ruseckas, G. Juzeliūnas, and I. V. Zozoulenko, Spectrum of $\pi$ electrons in bilayer graphene nanoribbons and nanotubes: An analytical approach, Phys. Rev. B **83**, 035403 (2011).

[18] K. Nakada, M. Fujita, G. Dresselhaus, and M. S. Dresselhaus, Edge state in graphene ribbons: Nanometer size effect and edge shape dependence, Phys. Rev. B **54**, 17954 (1996).

[19] M. Fujita, K. Wakabayashi, K. Nakada, and K. Kusakabe, Peculiar localized state at zigzag graphite edge, J. Phys. Soc. Jpn. **65**, 1920 (1996).

[20] J. Luck and Y. Avishai, Unusual electronic properties of clean and disordered zigzag graphene nanoribbons, J. Phys.: Condens. Matter **27**, 025301 (2015).

[21] L. Brey and H. A. Fertig, Elementary electronic excitations in graphene nanoribbons, Phys. Rev. B **75**, 125434 (2007).

[22] H. Hsu and L. E. Reichl, Selection rule for the optical absorption of graphene nanoribbons, Phys. Rev. B **76**, 045418 (2007).

[23] S. Ryu and Y. Hatsugai, Topological Origin of Zero-Energy Edge States in Particle-Hole Symmetric Systems, Phys. Rev. Lett. **89**, 077002 (2002).

[24] H. Zheng, Z. F. Wang, T. Luo, Q. W. Shi, and J. Chen, Analytical study of electronic structure in armchair graphene nanoribbons, Phys. Rev. B **75**, 165414 (2007).

[25] D. Klein, Graphitic polymer strips with edge states, Chem. Phys. Lett. **217**, 261 (1994).

[26] H. Chung, M. Lee, C. Chang, and M. Lin, Exploration of edge-dependent optical selection rules for graphene nanoribbons, Opt. Express **19**, 23350 (2011).

[27] M. Kohmoto and Y. Hasegawa, Zero modes and edge states of the honeycomb lattice, Phys. Rev. B **76**, 205402 (2007).

[28] H.-Y. Deng and K. Wakabayashi, Edge effect on a vacancy state in semi-infinite graphene, Phys. Rev. B **90**, 115413 (2014).

[29] S. Kasturirangan, A. Kamenev, and F. J. Burnell, Disordered graphene ribbons as topological multicritical systems, Phys. Rev. B **106**, 184206 (2022).